Fatigue and fracture toughness of Fe_3Al alloys with additions of Zr and C

M. Karlík*, A. Kubošová, P. Haušild, J. Prahl

Czech Technical University in Prague, Faculty of Nuclear Sciences and Physical Engineering, Department of Materials, Trojanova 13, 120 00 Prague 2, Czech Republic

Received 7 December 2007, received in revised form 7 February 2008, accepted 12 February 2008

Abstract

Fracture behaviour of two intermetallic alloys based on Fe_3Al with different Zr content was studied. On the alloy Fe-29.5Al-2.3Cr-0.63Zr-0.2C (at.%) (FA06Z), basic characterization of the microstructure by light and electron metallography was carried out. Tensile tests and fracture toughness tests were performed at 20, 200, 400, and 600 °C. The values of fracture toughness vary from 26 MPa $m^{1/2}$ (at 20 °C) to 42 MPa $m^{1/2}$ (at 400 °C). The fractographic analysis showed that the samples fractured at 20, 200 and 400 °C in the tensile or fracture toughness tests exhibit transgranular cleavage fracture, while the ductile dimple fracture predominates at 600 °C. Previous fatigue experiments on the alloy Fe-31.5Al-3.5Cr-0.25Zr-0.2C (at.%) (FA02Z) were completed by fatigue tests at 150 and 600 °C. The highest fatigue life and the lowest fatigue crack growth rates were found at 150 °C. The fatigue samples tested at all temperatures (20 to 600 °C) failed by transgranular cleavage fracture.

K e y w o r d s: iron aluminides, Fe_3Al, tensile test, fatigue crack growth, fracture toughness, fractographic analysis

1. Introduction

Iron aluminides based on Fe_3Al or FeAl are investigated as new high-temperature structural materials because of their low cost, low density, good wear resistance, ease of fabrication and superior resistance in oxidizing and sulfidizing atmospheres. These properties make them attractive as a lighter and potentially cheaper alternative to expensive (Cr-containing) stainless steels [1]. Iron aluminide-based alloys are expected to be used in components for coal energy conversion systems or furnaces for burning garbage, as cladding for boilers and heat exchangers, in the chemical industry, glass industry [2] and other applications as heating elements, furnace fixtures, heat-exchanger piping, sintered porous gas-metal filters, valve components, catalytic converter substrates and components for molten salt applications [3].

From the point of view of mechanical properties, the temperature about 540 °C is important for Fe_3Al-based alloys. At this temperature, $D0_3$-ordered structure (stable under 540 °C) is transformed to B2-ordered structure (stable above 540 °C) and vice versa. Unfortunately, the tensile and creep strength of Fe_3Al rapidly decrease in the B2-ordered structure, and the limiting temperature for its structural applications is around 600 °C [1, 4]. The results of numerous authors studying the high-temperature tensile and creep properties of iron aluminides were reviewed by Morris et al. [5, 6]. Main attention was paid to the influence of additives forming second-phase particles in Fe_3Al-type iron aluminides. This summary documents that the addition of Zr brings the best results since it forms a fine dispersion of carbides. Moreover, zirconium improves elongation at room temperature, and also shows a beneficial effect on the crack growth resistance [7, 8]. Very recently, Kratochvíl et al. [9] reported promising creep resistance results of one of the alloys (FA02Z) studied in this paper. Despite extensive research on iron aluminides, only little knowledge has been published on fracture toughness. It is the purpose of this paper to present results of fracture toughness determination carried out on another Fe_3Al-based material with 0.6 Zr and 0.2 C (at.%)

*Corresponding author: tel.: +420 224 358 507; fax: +420 224 358 532; e-mail address: Miroslav.Karlik@fjfi.cvut.cz

addition (FA06Z) in the range of temperatures from 20 to 600 ℃. Moreover, the results of the fatigue and fracture behaviour of the material FA02Z alloyed by 0.25 Zr and 0.2 C (at.%) [7] are extended up to 600 ℃.

2. Experimental details

Two Fe_3Al-based alloys with different Zr content (0.2 and 0.6 at.%) were prepared in VÚK – Kovohutě, s.r.o., Panenské Břežany (CZ) by vacuum induction melting and cast under argon atmosphere into copper mould with cross-section 38 mm × 120 mm. The ingots (about 12 kg in mass) were hot rolled at 1200 ℃ with 15 % thickness reduction in one pass. After each pass between the rolls, the material was reheated and at the final thickness it was rapidly cooled in the mineral oil. The plate for the alloy (FA02Z) was 7 mm thick (reduction in thickness 82 %), the alloy (FA06Z) was rolled to 13 mm thickness (reduction 65 %). Results of the chemical analysis of the alloys are in Table 1. After machining by milling, all the test specimens were annealed in air at 700 ℃ for 2 hours to relieve internal stresses and then quenched into mineral oil.

Basic material characterization of the FA02Z alloy, including static tensile tests carried out at temperatures 20 (RT), 200, 300, 400, 500, and 600 ℃ is reported in [7]. Microstructure characterization of the FA06Z alloy was performed using light and electron microscopy. Static tensile tests of the FA06Z alloy were carried out on INSTRON 1195 testing machine equipped with an atmospheric resistance-heated furnace. The cylindrical specimens having 5 mm in diameter, 26 mm gauge length and M12 threaded heads were tested at constant crosshead speed of 2 mm min^{-1} (initial strain rate $1.3 \times 10^{-3}\ s^{-1}$). The test temperature, measured by a thermocouple situated close to the specimen, was reached and stabilized within 2 hours.

Fatigue crack growth experiments of the FA02Z alloy at 150 and 600 ℃ were performed using compact tension (CT) specimens of thickness $B = 5$ mm and width $W = 40$ mm. The notch was produced by electro-discharge cutting using a wire 0.2 mm in diameter. The initial crack length a_o was 6.5 mm. The fatigue crack propagated perpendicularly to the rolling direction. The specimens were loaded in tension on a computer-controlled servohydraulic machine INOVA ZUZ 50 equipped with a resistance-heated furnace with electronic control of the test temperature within the range of ± 5 ℃ (fatigue tests at 20, 300 and 500 ℃ are reported in [7]). The frequency of loading was 10 Hz, the stress ratio R was 0.042 and the maximum load was 4.8 kN. The crack length during fatigue test was measured by (temperature independent) potential method at alternative current with the frequency of 4 Hz, using TECHLAB SRT-2K device, controlled by Fatigue Crack Growth Monitor software.

Table 1. Chemical composition of studied alloys

Alloy		Al	Cr	Zr	C	Fe
FA02Z	(at.%)	31.46	3.5	0.25	0.19	Balance
	(wt.%)	18.2	3.9	0.49	0.05	Balance
FA06Z	(at.%)	29.5	2.35	0.63	0.2	Balance
	(wt.%)	16.8	2.58	1.21	0.05	Balance

The fracture toughness tests of the FA06Z alloy were carried out on CT specimens having width $W = 25$ mm and thickness $B = 12.5$ mm. The specimens were loaded also on the computer-controlled servohydraulic loading machine INOVA ZUZ 50 equipped with a resistance-heated furnace. The fracture toughness tests were instrumented for measurement of J-integral. The crack extension during tests was measured by potential method. The crack propagated perpendicularly to the rolling direction. According to [10], the pre-crack was produced by electro-discharge cutting using a wire of 0.1 mm in diameter. Initial length was about $a = 14$ mm ($a/W = 0.55$). The use of notched samples instead of pre-cracked ones was confirmed on two specimens pre-cracked in fatigue in compliance with ASTM E 1820 standard. Both pre-cracking methods gave practically the same results (the number of test specimens was limited and so it was not possible to determine the experimental scatter). Eight full-thickness specimens and two pairs of specimens with reduced thickness (3.5 and 7.5 mm) were tested at room temperature. At elevated temperatures, two full-thickness specimens were tested at 200, 400 and 600 ℃.

Transmission electron micrographs were taken at JEOL EM 1200 microscope operated at 120 kV. Scanning electron microscope JEOL JSM 840A was used for the fractographic analysis. Micrographs were taken in the magnification range 10–20 000×.

3. Results and discussion

3.1. Microstructure

The microstructure of specimens machined from both hot-rolled plates (alloys FA02Z and FA06Z, which differ in the Zr content – 0.2 and 0.6 at.%, respectively), was recovered, with elongated grains in the rolling direction. The grains of the less Zr alloyed FA02Z material are large and relatively homogeneous in size (up to 1 mm in the direction of rolling and 300 μm in the transverse direction) and the grain boundaries are smooth. Moreover, there are no coarse particles visible on the light micrographs [7]. On the

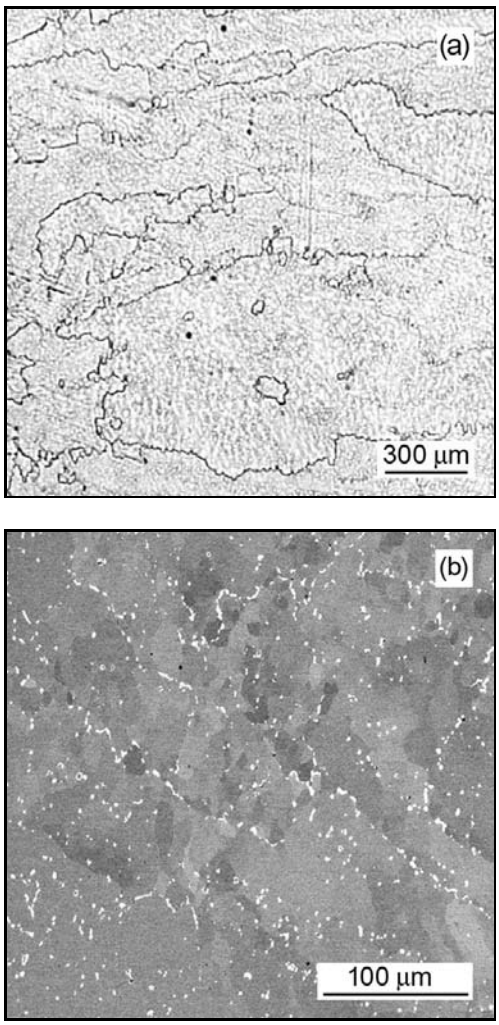

Fig. 1. (a) Light micrograph of Fe-28Al-2.3Cr-0.63Zr-0.2C (at.%) alloy (FA06Z) showing elongated grains in the rolling direction; (b) a dense distribution of coarse ZrC particles which appear bright in the backscattered electron signal.

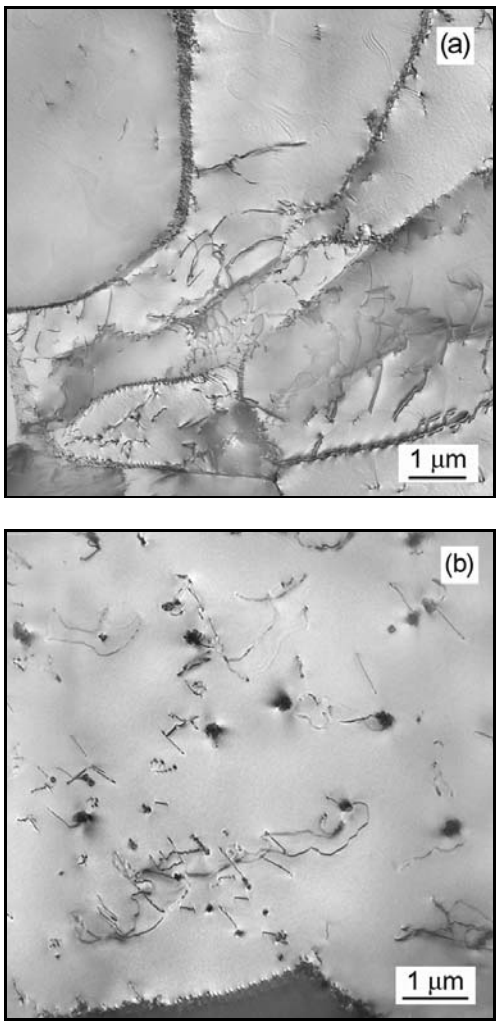

Fig. 2. TEM micrographs of Fe-28Al-2.3Cr-0.63Zr-0.2C alloy (FA06Z) showing subgrain boundaries (a) and fine ZrC particles in the matrix (b).

other hand, the grain size and the morphology of grain boundaries of the FA06Z alloy hot rolled with smaller reduction (65 %) are distinctly different. The grain size distribution is heterogeneous (Fig. 1a), with average values 500 μm and 200 μm in the longitudinal and transverse directions, respectively. However, grains 25 μm or 1 mm in size were also frequently observed. The grain boundaries are mostly ragged, very often with segments of a very low curvature (Fig. 1a). This is due to pinning by a dense array of ZrC particles (Fig. 1b), which effectively hinder the grain boundary motion during heating to the rolling temperature (1 100 ℃) and also during hot rolling itself. The size of these particles ranges from 0.5 to 7 μm. Some very coarse particles 30 μm in size were also observed.

If we compare transmission electron micrographs showing dislocation structure and finer particles, the differences are not so pronounced. The micrographs of FA02Z alloy were published elsewhere [11]. Both alloys have a well developed substructure, characteristic for a recovered material (Fig. 2a). The size of the subgrains ranges from 2 to 10 μm. The diffraction of backscattered electrons (EBSD) [12] showed that the disorientation of the subgrains was up to 5°. In both alloys, there are ZrC particles either in the subgrain boundaries or in the matrix (Fig. 2b). The distribution of these particles is not homogeneous in both alloys. There are relatively large regions with no particles at all. The only difference is in the size and density of particles. While the size of ZrC precipitates in the FA02Z alloy ranges from 30 to 50 nm [11], the smallest observed particles in the FA06Z alloy are usually coarser (100 to 250 nm). There are also particles 1 to 5 μm in diameter frequently observed in TEM micrographs [12].

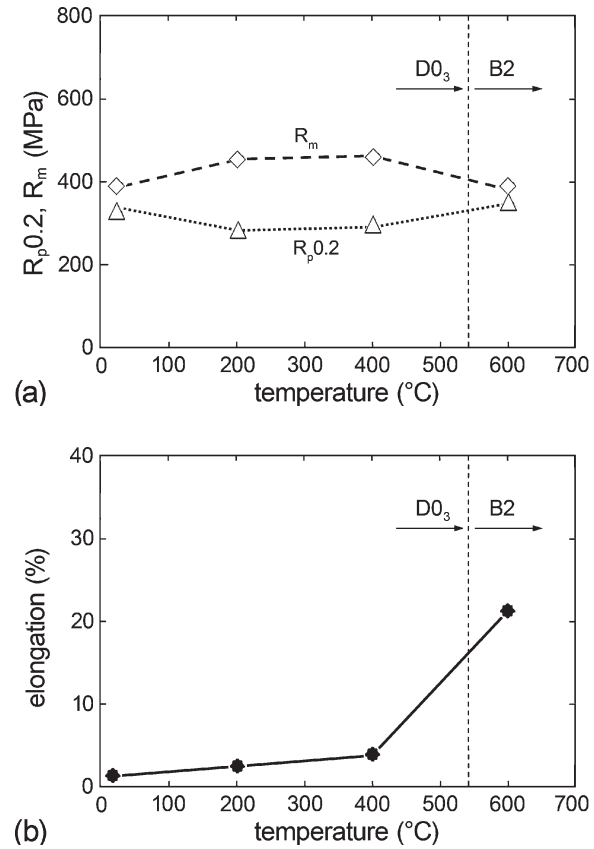

Fig. 3. Temperature dependences of 0.2 % proof stress, ultimate strength (a) and total elongation (b) for Fe-29.5Al-2.3Cr-0.63Zr-0.2C alloy (FA06Z).

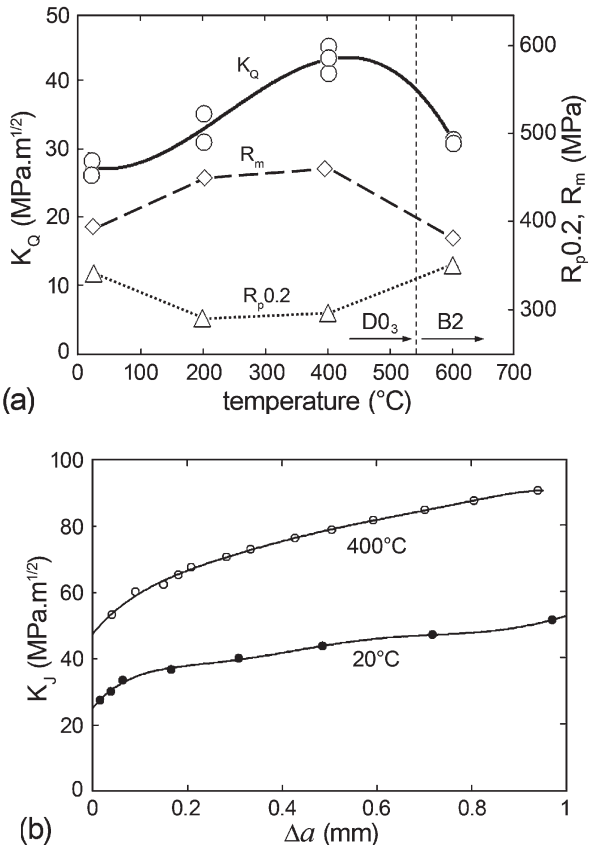

Fig. 4. Temperature dependences of K_Q, $R_p0.2$, R_m (a) and K_J vs. Δa plot (b) for Fe-29.5Al-2.3Cr-0.63Zr-0.2C alloy (FA06Z).

3.2. Static tensile tests

The basic mechanical characteristics, 0.2 % proof stress ($R_p0.2$), ultimate tensile strength (R_m) and tensile elongation (A), were measured at temperatures up to 600 °C. In the range from 20 to 540 °C ($D0_3$ region), $R_p0.2$ and R_m had their minimum at 200 °C (Fig. 3a). For both alloys (FA02Z and FA06Z), measured values at 20 and 400 °C were comparable and the values of $R_p0.2$ and R_m at 600 °C (B2 region) were practically identical. Tensile elongation at elevated temperatures in the $D0_3$ region was 3 to 4 times higher than at room temperature (1 %) and it considerably increased up to nearly 22 % in the B2 region (Fig. 3b). Described temperature dependences of tensile mechanical properties are in good agreement with the results measured on Fe-28Al-3.6Cr-0.1Ce-0.16C (at.%) alloy prepared under similar conditions [13].

3.3. Fracture toughness tests

At room temperature, the apparent fracture toughness K_Q of FA06Z alloy was 26 MPa m$^{1/2}$ (Fig. 4a). The values of fracture toughness evaluated from plots Load vs. Crack Opening Displacement (COD) were in good agreement with the values obtained from J-integral procedure. The limited thickness of specimens, B (given by the thickness of the hot-rolled plate) did not allow fulfilling of the condition (1) for measurement of the fracture toughness in the plane strain condition (K_{IC}):

$$B \geq 2.5 \left(\frac{K_Q}{R_p0.2} \right)^2 . \qquad (1)$$

However, the values of apparent fracture toughness K_Q were roughly independent on specimen thickness (for B = 3.5, 7.5, 12.5 mm).

The fracture toughness of FA06Z alloy increased from 26 MPa m$^{1/2}$ at 20 °C to 42 MPa m$^{1/2}$ at 400 °C and then decreased to about 31 MPa m$^{1/2}$ at 600 °C (Fig. 4a). Increasing resistance against crack growth with increasing temperature can also be seen in K_J-Δa curves (Fig. 4b) as an increasing slope of K_J.

3.4. Fractographic analysis

No differences were found in morphology of fracture surfaces comparing tensile and fracture tough-

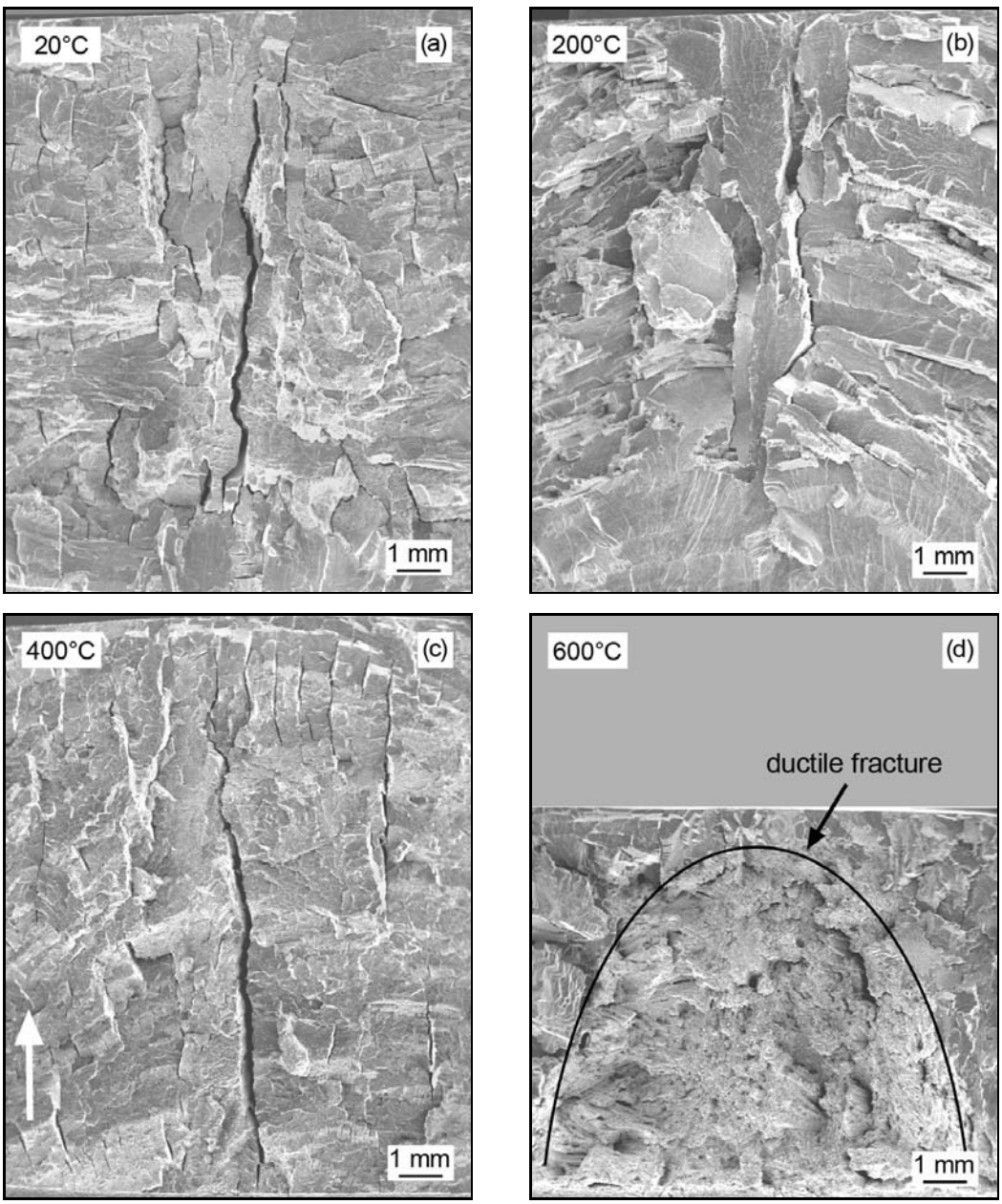

Fig. 5. General view of fracture surfaces of CT specimens from FA06Z alloy quasistatically tested at 20 °C (a), 200 °C (b), 400 °C (c), and 600 °C (d). The arrow in Fig. 5c shows direction of crack propagation.

ness specimens at the same testing temperature. The fractographic analysis showed that the specimens broken at 20, 200 and 400 °C exhibit transgranular cleavage fracture, while the ductile dimpled fracture predominates in experiments at 600 °C (Figs. 5, 6). The fracture surfaces contained secondary cracks oriented in perpendicular to the fracture surface (Figs. 5a,b,c, 6c), the highest number of these secondary cracks was found in specimens tested at 400 °C.

3.5. Fatigue crack growth experiments

The crack length a was measured during the fatigue tests as a function of elapsed number of loading cycles N. The fatigue crack growth rate $v = \mathrm{d}a/\mathrm{d}N$, determined by the secant method, is plotted in Fig. 7 as a function of a stress intensity factor range ΔK (calculated for the corresponding crack length a). Figure 7a shows (v-ΔK) plots at 150 and 600 °C, while Fig. 7b includes also results on the FA02Z alloy in the range from 20 to 500 °C from [7]. From Fig. 7a it is clearly seen, that fatigue crack growth rate at 600 °C is about two orders higher than at 150 °C for the same ΔK.

The temperature dependence of fatigue life (including crack initiation and propagation at a constant maximum load $F_{\max} = 4.8$ kN) is summarized in Table 2. The highest fatigue life was reached at 150 °C.

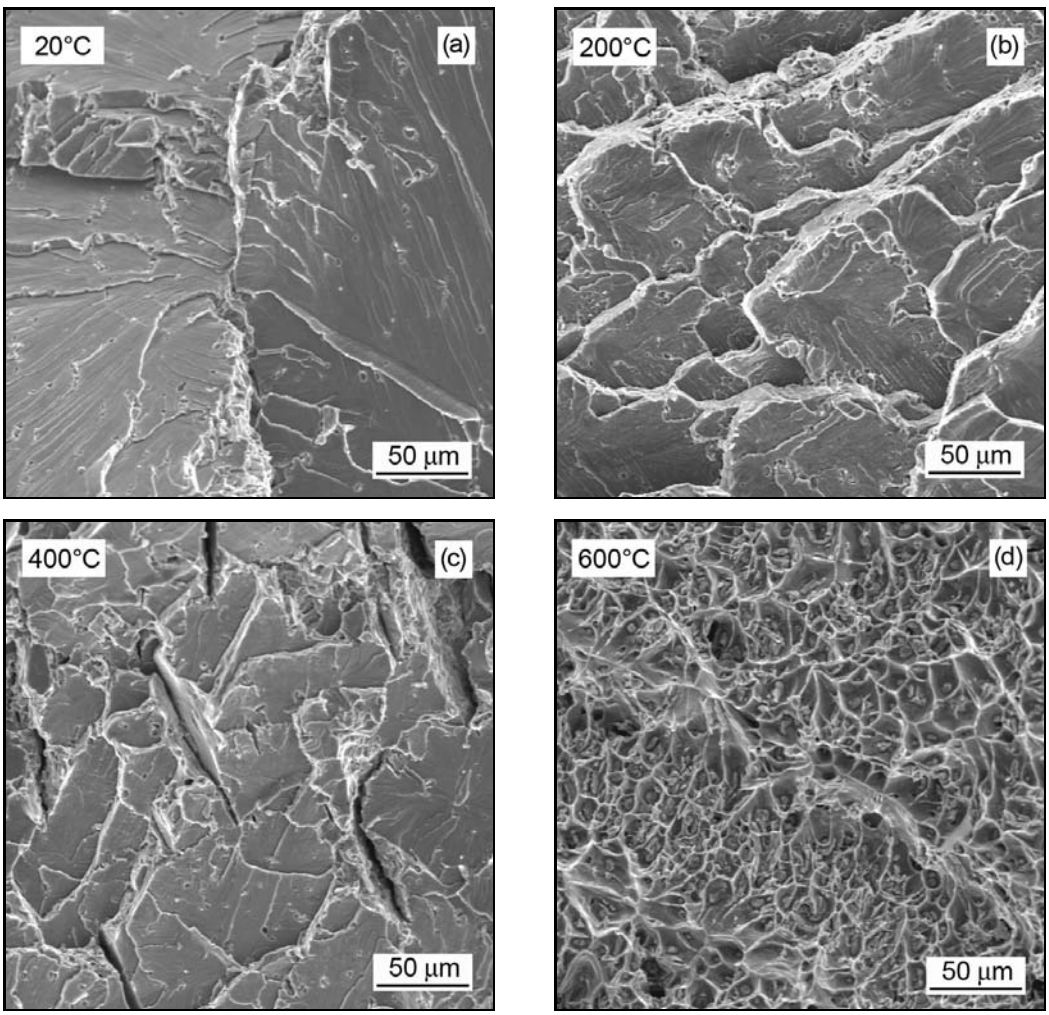

Fig. 6. Typical micromorphology of fracture of CT specimens from FA06Z alloy quasistatically tested at 20 °C (a), 200 °C (b), 400 °C (c) (cleavage) and 600 °C (d) (ductile dimples).

Table 2. Comparison of Paris exponent m, mean correlation coefficient r of $v(\Delta K)$ dependences and the number of cycles to failure N_f at different temperatures

t (°C)	20	150	300	500	600
m	8.1	3.9	2.1	2.4	3.0
r	0.74	0.71	0.92	0.96	0.93
N_f	245 000	480 000	228 000	6 000	4 400

The slope of $v(\Delta K)$ curves is much steeper (the exponent m in the Paris equation $v = C(\Delta K)^m$ is much higher) at 20 °C than at elevated temperatures. At elevated temperatures, the shape of the $v(\Delta K)$ curves is very similar. An important difference is in the fatigue crack growth rate: at 500 °C and 600 °C it is about two orders higher than at 150 °C and 300 °C.

The fatigue crack growth resistance of the alloy with Zr is higher than that of the similar alloy with Ce addition [7, 14].

3.6. Fractographic analysis – fatigue

The main fracture micromechanism is transgranular cleavage and it does not change significantly with increasing temperature. Fracture surfaces consist of facets varying in the arrangement, size and micromorphology. Most of the facets are common transgranular cleavage but also other types of facets were found (transgranular quasicleavage, intergranular decohesion, and, exceptionally, transgranular facets with ductile dimples). Some of the cleavage facets are covered by brittle fatigue striations (Fig. 8d). In addition, the fracture surface at 150 °C (Fig. 8a,b) (or at 500 °C [7]) in the $D0_3$-ordered structure was very similar to the fracture surface at 600 °C – in the B2-ordered structure – Fig. 8c,d. This means that the fracture mechanism under cyclic loading practically did not change during the transformation $D0_3 \leftrightarrow B2$. On the other hand, under static loading, after the transformation $D0_3 \leftrightarrow B2$, the transgranular cleavage changes to ductile dimpled fracture (Figs. 5, 6).

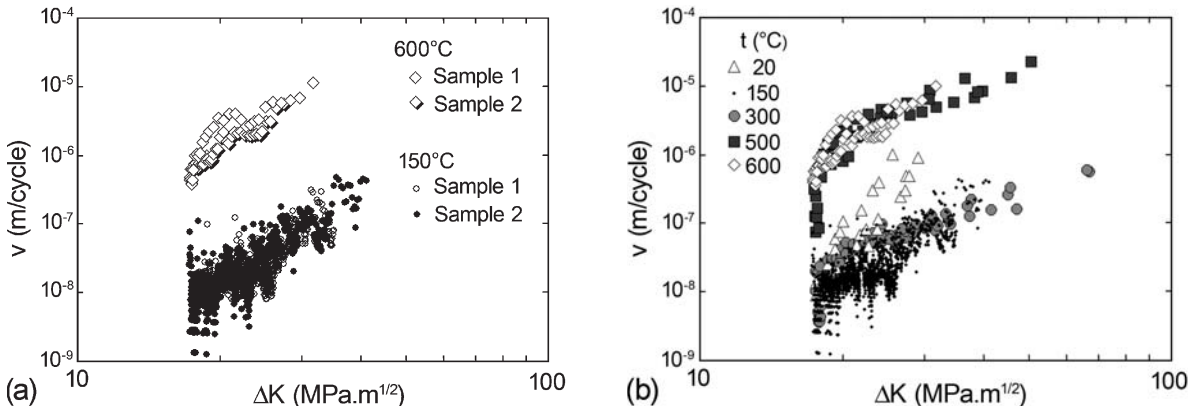

Fig. 7. Fatigue crack growth (v-ΔK) plots for Fe-31.5Al-3.5Cr-0.25Zr-0.2C (at.%) alloy (FA02Z) CT specimens tested (a) at 150 and 600 °C, (b) comparison with other results in the range from 20 to 500 °C [7].

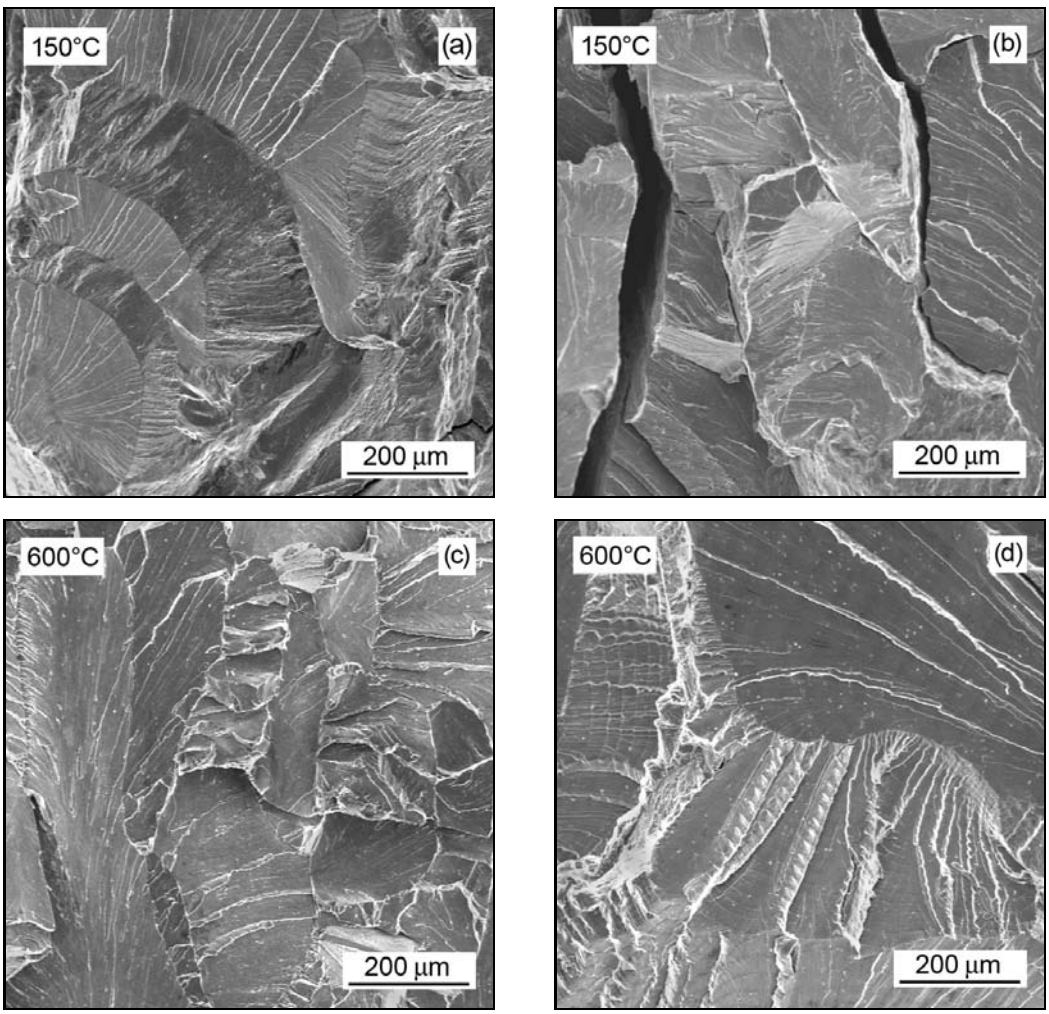

Fig. 8. Micromorphology of fracture of Fe-31.5Al-3.5Cr-0.25Zr-0.2C (at.%) alloy (FA02Z) tested in fatigue at 150 °C (a), (b) and 600 °C (c), (d).

4. Discussion

The fracture toughness tests of the FA06Z alloy were carried out mainly on specimens with spark cut notch having radius 120 to 160 µm. The reason for using only spark cut notch is a very similar character in the micromorphology of fatigue and static fracture surfaces of this specific material. A

detailed fractographic analysis of more than 10 fatigue tested specimens of Fe_3Al-based alloys [7, 10, 13, 14] has shown that it is practically impossible to recognize the boundary between fatigue crack and final rupture in the scanning electron microscope, because in both cyclic and static loading regime the material fails by transgranular cleavage. The only possibility how to distinguish the fatigue crack front is fatigue pre-cracking at elevated temperature (400 °C), during which the surface of the sample takes light brown colour allowing the observation of the crack front in the light microscope, however not in SEM.

After electro-discharge cutting, the initial crack opening was about $2c = 240$ to 320 μm. Since the ratio a/c varied from 42 to 58, the notch was considered as a narrow crack. In order to verify if the fracture toughness is influenced by the radius of the spark cut notch tip, two specimens pre-cracked in fatigue in compliance with ASTM E 1820 standard were also tested. Both pre-cracking methods gave practically the same results.

The results of fracture toughness tests at room temperature could be compared only with [10] where the fracture toughness was measured in the three-point bend test of 5 mm thick samples from Fe-28Al-3Cr alloy with Ce addition. The K_Q values measured at 20 °C were somewhat higher ($\sim 30\,\mathrm{MPa\,m^{1/2}}$).

Fatigue behaviour of FA02Z alloy at elevated temperatures is in agreement with Castagna and Stoloff [15] reporting similar results on Fe-28Al-5Cr-0.5Nb-0.2C (at.%) alloy at 150, 300 and 450 °C. Alven and Stoloff [8] measured fatigue crack growth rate on Fe_3Al-based alloys with different Zr and C addition, but only at room temperature.

As the results of static and cyclic mechanical properties that have been already obtained on various Fe_3Al-based materials alloyed by Ce or Zr [7, 10, 12–14, 16] were very similar, it is possible to compare the behaviour of alloys with somewhat different chemical composition in this paper. In other words it is fair to expect that FA06Z alloy would behave in the same manner in fatigue tests as the FA02Z alloy did. There is an interesting difference in the temperature dependence of the fracture behaviour of studied alloys during static and cyclic loading. In the static tests (tensile and fracture toughness) in the $D0_3$-ordered temperature region (up to 540 °C) the specimens fractured by transgranular cleavage fracture, while in experiments carried out at 600 °C (in the B2-ordered region) the ductile dimpled fracture predominated (Figs. 5, 6). On the other hand, in the cyclic loading micromorphology of the fracture does not change either with the crack length or with temperature, even at the temperature 600 °C, above the $D0_3$-B2 transition (Fig. 8). The micromorphology of fracture of Fe_3Al-based alloys during cyclic loading in air is transgranular cleavage. The reason for this behaviour could be the extrinsic character of the brittleness of this material, caused by hydrogen [17, 18]. During cyclic loading, hydrogen formed at the surface of the test specimen has enough time to diffuse to the stress field of the crack tip, where it influences the failure of the material. On the other hand, the rate of loading during tensile or fracture toughness test is so high that hydrogen formed at the surface of the test specimen could not influence the failure in the same manner as during fatigue test. According to [8] hydrogen moves into the lattice ahead of the fatigue crack tip by a dislocation-assisted transport mechanism.

5. Conclusions

1. The basic characterization of the microstructure and mechanical properties of Fe-29.5Al-2.3Cr-0.63Zr-0.2C (at.%) (FA06Z) alloy showed that this material with higher Zr content had similar properties compared to other Fe_3Al-based alloys with Ce or Zr addition prepared in similar conditions.

2. The values of fracture toughness evaluated from plots Load vs. Crack Opening Displacement (COD) were in good agreement with the values obtained from *J*-integral procedure.

3. The conditions for measuring the fracture toughness in the plane strain condition (K_{IC}) were not fulfilled due to higher fracture toughness and limited thickness of specimens. However, the values of fracture toughness at room temperature K_Q were roughly independent on specimen thickness (for 3.5, 7.5, 12.5 mm).

4. The fracture toughness of FA06Z alloy increased from $26\,\mathrm{MPa\,m^{1/2}}$ at 20 °C to $42\,\mathrm{MPa\,m^{1/2}}$ at 400 °C and then decreased to about $31\,\mathrm{MPa\,m^{1/2}}$ at 600 °C.

5. No differences were found in morphology of fracture surfaces comparing tensile and fracture toughness specimens at the same testing temperature. The fractographic analysis showed that the specimens fractured at 20, 200 and 400 °C exhibit transgranular cleavage fracture, while in experiments at 600 °C the ductile dimpled fracture predominates.

6. The highest fatigue life, nearly 500 000 cycles, was measured at 150 °C for the 31.5Al-3.5Cr-0.25Zr-0.2C (at.%) (FA02Z) alloy.

7. The crack growth rate in FA02Z alloy at 600 °C practically did not change when compared to that at 500 °C. Even if the material at 600 °C is B2-ordered, the micromechanism of failure in cyclic loading – transgranular cleavage – did not change as in the case of static loading (tensile and fracture toughness tests), where transgranular cleavage changes in the B2 region to ductile dimpled fracture. This difference is probably due to hydrogen diffusion ahead of the fatigue crack tip by a dislocation-assisted transport mechanism.

Acknowledgements

Financial support from the Czech Ministry of Education, Youth and Sports (project MSM6840770021) is gratefully acknowledged.

References

[1] STOLOFF, N. S.: Mater. Sci. Eng., *A258*, 1998, p. 1.
[2] HOTAŘ, A.—KRATOCHVÍL, P.: Intermetallics, *15*, 2007, p. 439.
[3] DEEVI, S. C.—ZHANG, W. J.: Applications of Intermetallics. Encyclopaedia of Materials. Amsterdam, Elsevier 2005.
[4] WESTBROOK, J. H.—FLEISHER, R. L.: Intermetallic Compounds. New York, John Wiley 1995.
[5] MORRIS, D. G.—MUNOZ-MORRIS, M. A.—CHAO, J.: Intermetallics, *12*, 2004, p. 821.
[6] MORRIS, D. G.—MUNOZ-MORRIS, M. A.—BAUDIN, C.: Acta Mater., *52*, 2004, p. 2827.
[7] PRAHL, J.—HAUŠILD, P.—KARLÍK, M.—CRENN, J.-F.: Kovove Mater., *43*, 2005, p. 134.
[8] ALVEN, D. A.—STOLOFF, N. S.: Mater. Sci. Eng., *A239–240*, 1997, p. 362.
[9] KRATOCHVÍL, P.—MÁLEK, P.—CIESLAR, M.—HANUS, P.—HAKL, J.—VLASÁK, T.: Intermetallics, *15*, 2007, p. 333.
[10] HAUŠILD, P.—KARLÍK, M.—SIEGL, J.—NEDBAL, I.: Intermetallics, *13*, 2005, p. 217.
[11] CIESLAR, M.—KARLÍK, M.: Mater. Sci. Eng., *A462*, 2007, p. 289.
[12] KUBOŠOVÁ, A.: Fracture behaviour of ordered alloys based on Fe_3Al. [Diploma work]. Prague, Czech Technical University in Prague 2006 (in Czech).
[13] HAUŠILD, P.—KARLÍK, M.—NEDBAL, I.—PRAHL, J.: Kovove Mater., *42*, 2004, p. 156.
[14] KARLÍK, M.—NEDBAL, I.—SIEGL, J.—PRAHL, J.: Journal of Alloys and Compounds, *378*, 2004, p. 263.
[15] CASTAGNA, A.—STOLOFF, N. S.: Mater. Sci. Eng., *A192–193*, 1995, p. 399.
[16] KARLÍK, M.—NEDBAL, I.—SIEGL, J.—LAUSCHMANN, H.—PRAHL, J.—ČERNOCH, T.: In: Proceedings of Fatigue Crack Paths 2003. Eds.: Carpinteri, A., Cook, L. P. Parma (Italy), University of Parma, 2003, p. 1.
[17] LIU, C. T.—LEE, E. H.—McKAMEY, C. G.: Scripta Metall. Mater., *23*, 1989, p. 875.
[18] LIU, C. T.—McKAMEY, C. G.—LEE, E. H.: Scripta Metall. Mater., *24*, 1990, p. 385.